MOLECULAR AND CELLULAR BIOLOGY, Jan. 2004, p. 1–13 Vol. 24, No. 1
0270-7306/04/$08.00+0 DOI: 10.1128/MCB.24.1.1–13.2004

Disturbed Cholesterol Homeostasis in a Peroxisome-Deficient *PEX2* Knockout Mouse Model

Werner J. Kovacs,[1] Janis E. Shackelford,[1] Khanichi N. Tape,[1] Michael J. Richards,[2] Phyllis L. Faust,[3] Steven J. Fliesler,[2] and Skaidrite K. Krisans[1]*

Department of Biology, San Diego State University, San Diego, California 92182[1]; Saint Louis University Eye Institute and Department of Pharmacological and Physiological Sciences, Saint Louis University School of Medicine, St. Louis, Missouri 63104[2]; and Department of Pathology, Columbia University, New York, New York 10027[3]

Received 27 June 2003/Returned for modification 2 September 2003/Accepted 18 September 2003

We evaluated the major pathways of cholesterol regulation in the peroxisome-deficient *PEX2*$^{-/-}$ mouse, a model for Zellweger syndrome. Zellweger syndrome is a lethal inherited disorder characterized by severe defects in peroxisome biogenesis and peroxisomal protein import. Compared with wild-type mice, *PEX2*$^{-/-}$ mice have decreased total and high-density lipoprotein cholesterol levels in plasma. Hepatic expression of the SREBP-2 gene is increased 2.5-fold in *PEX2*$^{-/-}$ mice and is associated with increased activities and increased protein and expression levels of SREBP-2-regulated cholesterol biosynthetic enzymes. However, the upregulated cholesterogenic enzymes appear to function with altered efficiency, associated with the loss of peroxisomal compartmentalization. The rate of cholesterol biosynthesis in 7- to 9-day-old *PEX2*$^{-/-}$ mice is markedly increased in most tissues, except in the brain and kidneys, where it is reduced. While the cholesterol content of most tissues is normal in *PEX2*$^{-/-}$ mice, in the knockout mouse liver it is decreased by 40% relative to that in control mice. The classic pathway of bile acid biosynthesis is downregulated in *PEX2*$^{-/-}$ mice. However, expression of CYP27A1, the rate-determining enzyme in the alternate pathway of bile acid synthesis, is upregulated threefold in the *PEX2*$^{-/-}$ mouse liver. The expression of hepatic ATP-binding cassette (ABC) transporters (ABCA1 and ABCG1) involved in cholesterol efflux is not affected in *PEX2*$^{-/-}$ mice. These data illustrate the diversity in cholesterol regulatory responses among different organs in postnatal peroxisome-deficient mice and demonstrate that peroxisomes are critical for maintaining cholesterol homeostasis in the neonatal mouse.

Cholesterol is an essential structural constituent of cellular membranes and a precursor molecule for the synthesis of steroid hormones, bile acids, and regulatory oxysterols. Cholesterol homeostasis is achieved by a series of regulatory steps that control cholesterol biosynthesis, its uptake from plasma lipoproteins, and the conversion of cholesterol to bile acids (27, 45). The prevailing view has been that cholesterol biosynthetic reactions occur in the cytoplasm and endoplasmic reticulum. However, recent studies suggest that the early steps in the isoprenoid/cholesterol biosynthetic pathway occur in peroxisomes, since all of the enzymes required for the conversion of acetyl coenzyme A (acetyl-CoA) to farnesyl diphosphate (FPP) are localized in peroxisomes and the enzymes catalyzing the conversion of mevalonate to FPP appear to be exclusively peroxisomal (30). Proteins imported into the peroxisome matrix use either C-terminal tripeptide (PTS 1) or N-terminal nonapeptide (PTS 2) peroxisome targeting signals that are recognized by the cytosolic receptors Pex5p and Pex7p, respectively (40). Both peroxisomal import pathways are utilized by peroxisomal cholesterol biosynthetic enzymes, and PTS1 and PTS2 are found in an alternating order (30). 3-Hydroxy-3-methylglutaryl (HMG) CoA reductase, localized in the endoplasmic reticulum and peroxisomes, is the only enzyme in the cholesterol biosynthetic pathway required for the conversion of HMG-CoA to mevalonate for which we, as yet, have no peroxisomal targeting information.

The importance of peroxisomes for normal cellular functioning is illustrated by the disorders associated with the Zellweger spectrum (Zellweger syndrome [ZS], neonatal adrenoleukodystrophy and infantile Refsum's disease). All of these diseases are characterized by a loss of functional peroxisomes resulting in the presence of matrix enzymes in the cytosol (21). In Zellweger syndrome (ZS), the most severe of these disorders, infants have central nervous system neuronal migration defects associated with neonatal hypotonia, seizures, and hepatic dysfunction.

The effect of peroxisomal dysfunction on cholesterol biosynthesis in cells and tissues from patients with the Zellweger spectrum disorders has been examined, with conflicting results (30). Briefly, reduced plasma cholesterol levels have been found in Zellweger spectrum patients (30). Normal enzyme activities for mevalonate kinase (MvK), mevalonate diphosphate decarboxylase (MPD), and isopentenyl diphosphate isomerase (IPPI) have been measured in fibroblasts from ZS patients in one study (54), but decreased MvK activity was found in fibroblasts from ZS and neonatal adrenoleukodystrophy patients in another study (6). While three groups reported significantly decreased cholesterol biosynthesis in fibroblasts from Zellweger spectrum patients (25, 34; J. C. Collins, F. Keyserman, S. C. Rumsey, and R. J. Deckelbaum, Am. Heart Assoc. abstr. 1219, PG I-228, 1993), two other studies showed

* Corresponding author. Mailing address: Department of Biology, San Diego State University, 5500 Campanile Dr. LS-331, San Diego, CA 92182. Phone: (619) 594-5368. Fax: (619) 594-5676. E-mail: skrisans@sunstroke.sdsu.edu.

that cholesterol biosynthesis rates were equivalent to or slightly higher than those in control fibroblasts (33, 37). A study by Krisans et al. (31) analyzing liver samples from Zellweger spectrum patients has shown that enzymatic activities of HMG-CoA reductase, MvK, phosphomevalonate kinase, MPD, IPPI, and FPP synthase were reduced, while another group reported decreased or normal MvK activities in livers of ZS patients (54). In addition, one group reported a decrease in cholesterol biosynthesis in peroxisome-deficient *PEX2*$^{-/-}$ hamster cells (1), while another group reported increased cholesterol biosynthesis in the same cell lines (52).

Recently, peroxisome-deficient mouse models for human ZS have become available for study. In one such model, the *PEX5* knockout mouse, the cholesterol biosynthesis rate was normal in immortalized as well as primary *PEX5*$^{-/-}$ mouse fibroblast cultures (53). Cholesterol levels were also normal in the plasma, brain, and liver of newborn *PEX5*$^{-/-}$ mice, while hepatic enzyme activities for HMG-CoA reductase and IPP isomerase were slightly elevated (26). These *PEX5*-deficient mice die within 24 h after birth and thus cannot be used to study postnatal effects (2).

The second mouse model for human ZS has a targeted deletion of the *PEX2* gene (13), and homozygous mutants survive in the early postnatal period up to 13 days (12, 14). Thus, the *PEX2* mouse provides an excellent model to assess the effect of peroxisomal deficiency on cholesterol homeostasis in the early postnatal period.

The focus of our study was to characterize the effects of peroxisome deficiency on an array of cholesterol biosynthetic enzymes, bile acid proteins, ATP-binding cassette (ABC) transporters, transcription factors, and nuclear receptors that are involved in maintaining cholesterol homeostasis. Our data illustrate that the loss of peroxisomes leads to an upregulation of the sterol regulatory element-binding protein 2 (SREBP-2) pathway in the liver and a corresponding increase in the activities and the protein and expression levels of SREBP-2-regulated cholesterol biosynthetic enzymes. However, due to the loss of compartmentalization, the cholesterol biosynthetic enzymes function with altered catalytic efficiency. The rate of cholesterol biosynthesis is increased in most tissues, except in the brain and kidneys, where it is reduced. The cholesterol contents of all tissues examined were found to be similar in wild-type and *PEX2* knockout mice, with the exception of the liver, where the cholesterol content is significantly reduced in the *PEX2* knockout mice. In addition, compared with wild-type mice, *PEX2*$^{-/-}$ mice have decreased plasma total and high-density lipoprotein (HDL) cholesterol levels. The classic pathway of bile acid biosynthesis is downregulated, while the alternate pathway is unexpectedly increased. Our studies demonstrate that there is a loss of coordinate regulation of cholesterol homeostasis in the *PEX2* knockout mice and emphasize the importance of the peroxisome in this process.

MATERIALS AND METHODS

Generation of *PEX2*-deficient mice. Homozygous *PEX2*$^{-/-}$ mice were obtained by breeding *PEX2* heterozygotes (Swiss Webster [SW] × 129SvEv murine genetic background) (12, 14) and genotyped by PCR analysis of tail DNA (13). Mice had access to food and water ad libitum and were exposed to a 12-h light-dark cycle in a temperature-controlled room (22°C).

Plasma and hepatic lipid analysis. Plasma total cholesterol and HDL cholesterol levels were measured by an enzymatic assay using a commercial kit (Sigma, St. Louis, Mo). Tissue sterol levels were determined by reverse-phase high-performance liquid chromatography (HPLC) after saponification and petroleum ether extraction, as described previously (16, 17). Plasma phospholipid and triglyceride levels were determined enzymatically (WAKO Chemicals, Neuss, Germany). The plasma low-density lipoprotein (LDL) cholesterol level was calculated from the Friedewald formula, applying the values for total cholesterol, HDL cholesterol, and triglycerides (18).

Enzyme assays. Catalase (EC 1.11.1.6) activity was measured by the method of Baudhuin et al. (4). HMG-CoA reductase (EC 1.1.1.34) activity was determined as described previously (11), except that the KEND buffer contained 0.5% (vol/vol) Triton X-100 and the samples (100 μg of protein) were incubated at 37°C for 40 min. FPP synthase (EC 2.5.1.1) activity was assayed for 45 min using 10 μg of protein and [^{14}C]IPP (18 mCi/mmol; American Radiolabeled Chemicals, St. Louis, Mo.) as described previously (23). Squalene synthase (EC 2.5.1.21) activity was assayed for 60 min using 20 μg of protein and [^{3}H]FPP (150 mCi/mmol; American Radiolabeled Chemicals) as described previously (50).

IPP isomerase (EC 5.3.3.2) activity was assayed as follows. The reaction buffer consisted of 50 mM HEPES, 20 mM $MgCl_2$, and 10 mM dithiothreitol (pH 7.0). Each 0.1-ml sample contained 12.5 nmol of [^{14}C]IPP (275,000 cpm; American Radiolabeled Chemicals). The samples were incubated at 37°C, and the reactions were terminated by addition of 0.4 ml 25% HCl in methanol. [^{3}H]FPP standard (17,000 cpm) was then added to each sample, and the reaction mixtures were incubated 10 min at 37°C. The reaction mixtures were saturated with NaCl, the products were extracted twice with a total of 4 ml of hexane, and the hexane phase was counted by liquid scintillation.

Protein concentrations were determined by the bicinchoninic acid method (Pierce, Rockford, Ill.) using bovine serum albumin as a standard.

Western blot analysis. Proteins were separated on a sodium dodecyl sulfate (SDS)–13% polyacrylamide gel and transferred to nitrocellulose. Immunoblot analysis was performed using enhanced chemiluminescence immunodetection (NEN ECL detection reagents; PerkinElmer Life Sciences, Boston, Mass.) with the following antibodies: anticatalase (a gift of A. Voelkl, University of Heidelberg), anti-(acyl-CoA oxidase) (a gift of A. Voelkl), anti-(HMG-CoA reductase) (a gift of P. Edwards), anti-MvK, anti-IPPI, and anti-(FPP synthase) (a gift of P. Edwards), with the appropriate horseradish peroxidase-linked secondary antibody (Bio-Rad, Hercules, Calif.). Rabbit polyclonal antiserum was raised against a 15-amino-acid peptide corresponding to mouse IPP isomerase (residues 209 to 223, CDNLNHLSPFVDHEK). Blots were exposed to X-OMAT LS films (Eastman Kodak Co., Rochester, N.Y.). Films were scanned on a Molecular Dynamics personal densitometer and analyzed using ImageQuant software (Amersham Pharmacia Biotech, Piscataway, N.J.).

Northern blot analysis. Total RNA was isolated using Trizol reagent (Invitrogen, Carlsbad, Calif.), and poly(A)$^+$ RNA was further purified using the PolyATtract mRNA isolation system (Promega, Madison, Wis.). RNA was quantitated by optical densitometry at 260 nm and subjected to electrophoresis on a formaldehyde–1.0% agarose gel. After separation, the RNA was transferred to Hybond-XL membranes (Amersham Pharmacia Biotech, Piscataway, N.J.) and fixed by UV cross-linking.

cDNA probes were prepared from mouse liver total RNA by a standard reverse transcriptase-PCR (Invitrogen) procedure using primers based on mouse cDNA sequences available through GenBank databases. PCR-generated probes were subcloned into the pCRII-TOPO vector (Invitrogen), sequenced, released from the cloning vector with restriction enzymes, and purified by agarose gel electrophoresis before being radiolabeled by the nick translation method (Roche, Indianapolis, Ind.) using [α-^{32}P]dCTP (Perkin-Elmer Life Sciences). Probe hybridization was carried out overnight at 42°C in a solution containing 50% (vol/vol) formamide, 0.75 M NaCl, 75 mM sodium citrate (pH 7.0), 2x Denhardt's solution, 0.1% SDS, 200 μg of salmon sperm DNA per ml, and 10% dextran sulfate. Washes (two with 15 min each) were performed at 42°C using 2x SSC (1x SSC is 0.15 M NaCl plus 0.015 M sodium citrate)–0.1% SDS, 0.5x SSC–0.1% SDS, and 0.2x SSC–0.1% SDS. Blots were exposed to PhosphorImager screens and visualized using a Storm 860 PhosphorImager system (Molecular Dynamics, Sunnyvale, Calif).

Forward and reverse PCR primers used to generate cDNA probes were, respectively, as follows (GenBank accession numbers are provided in parentheses): phosphomevalonate kinase (AK003607), 5′-AAATCCGGGAAGGACTTCGT-3′ and 5′-TTGCTGTCGACTCTGCTCCG-3′; IPP isomerase (AF003835), 5′-AGGAGTGATTGGATCAGCTC-3′ and 5′-AACTTAATTTCGCCCCTGGC-3′; FPP synthase (M34477), 5′-AGAATGAATGGGGACCAGAA-3′ and 5′-AGGTTACTTTCTCCGCTTGT-3′; 7-dehydrocholesterol reductase (AF057368), 5′-TTGTGTACTACTTCATCATGGCATG-3′ and 5′-GGGTTGAACTCAAT

TABLE 1. Plasma lipid analysis of 10-day-old wild-type and *PEX2* knockout mice

Lipid	Lipid concn (mg/dl) in[a]:		Ratio of lipid concns
	Wild-type mice	*PEX2*$^{-/-}$ mice	
Total plasma cholesterol	191.3 ± 26.7 (14)	109.5 ± 33.7 (6)*	0.57
Total plasma HDL cholesterol	96.1 ± 19.4 (14)	25.7 ± 10.5 (6)*	0.27
Plasma triglycerides	69.7 ± 26.5 (26)	77.4 ± 21.0 (7)	1.11
Plasma phospholipids	430.1 ± 52.6 (19)	285.7 ± 60.5 (7)*	0.66

[a] Each value represents the mean ± standard error of the mean. Values in parentheses denote the number of samples analyzed. *, $P < 0.001$ (Student's *t* test).

TCCCATCAT-3′; lanosterol synthase (U31352), 5′-TGGCTGGCTGTCCTGA ATGTTTA-3′ and 5′-TTGGTGCCCTGCATTTTCAT-3′; cytochrome P450 3A11 (CYP3A11) (NM_007818.1), 5′-TTTTCTGTCTTCACAAACCGG-3′ and 5′-CAAACCTCATGCCAAGGCAG-3′; insig-1, 5′-AGGACGACAGTTAGCT ATGGGTG-3′ and 5′-CCCCCTTACCCGACTCTCACATAC-3′; and insig-2, 5′-CTGGTGTGCCTTTTCCCGTTTCTA-3′ and 5′-ACCTTGATCTGCCTGT GTTCCTGT-3′.

In vivo cholesterol synthesis. Neonatal mice were injected with sodium [^{3}H]acetate (25 Ci/mmol; American Radiolabeled Chemicals) in sterile phosphate-buffered saline (135 mCi/ml; 0.676 mCi/g of body weight) under the dorsal skin, using a Hamilton syringe fitted with a 30-gauge needle. After metabolism of the radiolabeled substrate was allowed to proceed for 6 h, the mice were euthanized and tissues were harvested, weighed, flash frozen in liquid nitrogen, and stored at −85°C until ready for analysis. Blood was collected by intracardiac puncture, and plasma was prepared by centrifugation (5 min at 10,000 × *g*); an aliquot (5 μl) was taken for scintillation counting, while another aliquot (20 to 25 μl) was taken for determination of sterol specific activity. Following saponification and petroleum ether extraction, the nonsaponifiable lipids were analyzed by reverse-phase radio-HPLC, and the specific activities of the radiolabeled products (e.g., sterols, squalene) were determined as previously described (16).

RESULTS

Plasma lipid analysis of wild-type and *PEX2*$^{-/-}$ mice. We first investigated if peroxisome-deficient mice had any abnormalities in plasma lipids. The plasma total cholesterol and HDL cholesterol levels were reduced 43 and 73%, respectively, in 10-day-old *PEX2*$^{-/-}$ mice (Table 1). The plasma phospholipid level was reduced by 34% in *PEX2*$^{-/-}$ mice compared with their controls. There was no significant difference between *PEX2*$^{-/-}$ and wild-type mice in plasma triglyceride levels. The calculated plasma LDL cholesterol concentration in wild-type and *PEX2*$^{-/-}$ mice was 81.3 and 68.3 mg/dl, respectively. In the C57BL/6 background newborn *PEX2* knockout mice, total plasma cholesterol and phospholipid levels were also reduced by approximately 40% (data not shown).

Cholesterol biosynthetic enzyme activities are markedly increased in livers of *PEX2*$^{-/-}$ mice. To examine the effect of peroxisome deficiency on the activities of cholesterol biosynthetic enzymes, we measured the activities of HMG-CoA reductase, IPP isomerase, FPP synthase, and squalene synthase in liver homogenates of *PEX2* knockout, heterozygous, and wild-type mice from postnatal days 0.5 (P0.5), 3 to 5 (P3–5), and 7 to 10 (P7–10). HMG-CoA reductase is normally localized in both the endoplasmic reticulum and peroxisomes, IPP isomerase and FPP synthase are localized predominantly in peroxisomes, while squalene synthase is localized exclusively in the endoplasmic reticulum.

While the activity of these enzymes in the newborn *PEX2*$^{-/-}$ mouse liver was normal, all enzyme activities were significantly elevated in the postnatal knockout mouse livers (Fig. 1A to D). In control mice, the activity of these cholesterol biosynthetic enzymes was highest at P0.5 and decreased over the subsequent 10-day period (Fig. 1A to D). The pattern observed in *PEX2* knockout mice differed markedly, with enzyme activity continuing to increase in postnatal *PEX2*$^{-/-}$ mice. For example, HMG-CoA reductase activity was increased 5-fold at P3–5 and 10-fold at P7–10 in knockout mice (Fig. 1A). Activities of IPP isomerase, FPP synthase, and squalene synthase were increased twofold at P3–5 in *PEX2*$^{-/-}$ mice (Fig. 1B to D). At P7–10, the activities of FPP synthase and squalene synthase were increased 10-fold in mutant mice while IPP isomerase activity was increased 18-fold.

In the livers of newborn mice, the activity of catalase, the marker enzyme of peroxisomes, was similar for *PEX2*$^{-/-}$ and control mice (Fig. 1E). However, at P3–5 and P7–10, the catalase activity in liver homogenates of *PEX2*$^{-/-}$ mice was only half that in their wild-type littermates (Fig. 1E).

Activities of selected cholesterol biosynthetic enzymes in the kidneys and spleen of *PEX2*$^{-/-}$ mice. Prompted by our data showing highly elevated activities of cholesterol biosynthetic enzymes in the livers of ZS mice, we also investigated the enzyme activities in the kidneys and spleen of 10-day-old wild-type and *PEX2*$^{-/-}$ mice (Table 2). In the spleen of *PEX2*$^{-/-}$ mice the activities of HMG-CoA reductase, IPP isomerase, and FPP synthase were increased twofold as compared to those in wild-type mice. Therefore, there is a similar pattern of enzyme elevation to that observed in the *PEX2* knockout liver, which is somewhat less extensive in the spleen. In the *PEX2*$^{-/-}$ mouse kidneys, the pattern of enzyme alterations differed significantly from that in liver or spleen. Whereas activities of FPP synthase and squalene synthase were increased around twofold, as in spleen, the specific activity of HMG-CoA reductase was decreased twofold, and the activity of IPP isomerase was unchanged in *PEX2*$^{-/-}$ mouse kidneys. This finding suggests a differential regulation of cholesterol homeostasis in the *PEX2*$^{-/-}$ mouse kidneys from that in the liver or spleen.

Protein levels of cholesterol biosynthetic enzymes are markedly increased in the livers of PEX2$^{-/-}$ mice. Western blot analysis of peroxisomal proteins and proteins involved in cholesterol biosynthesis was performed to determine whether the measured activities are a reflection of the protein levels. Acyl-CoA oxidase is a peroxisomal protein that undergoes proteolytic cleavage after import into peroxisomes (36). While the level of this enzyme increased in the postnatal period in both control and mutant mice, only the uncleaved subunit A was seen in *PEX2*$^{-/-}$ mouse livers, consistent with the lack of peroxisomal protein import in knockout mice (Fig. 2). The amount of catalase in livers of P7–10 *PEX2*$^{-/-}$ mice was decreased to 70% of control levels, which is consistent with the reduced catalase activity in the *PEX2*$^{-/-}$ mice (Fig. 2B; also see Fig. 1E). Similar protein levels of most cholesterol biosynthetic enzymes were seen in P0.5 wild-type, *PEX2* heterozygous, and *PEX2*$^{-/-}$ mouse livers, with the exception of IPP isomerase, whose level was increased by twofold (Fig. 2A). Figure 2B illustrates the protein levels of a number of cholesterol biosynthetic enzymes in livers of P7–10 mice. The protein levels were significantly elevated in *PEX2*$^{-/-}$ mice, but the magnitude of the increase varied widely between different knockout mice. However, a similar wide variation was also

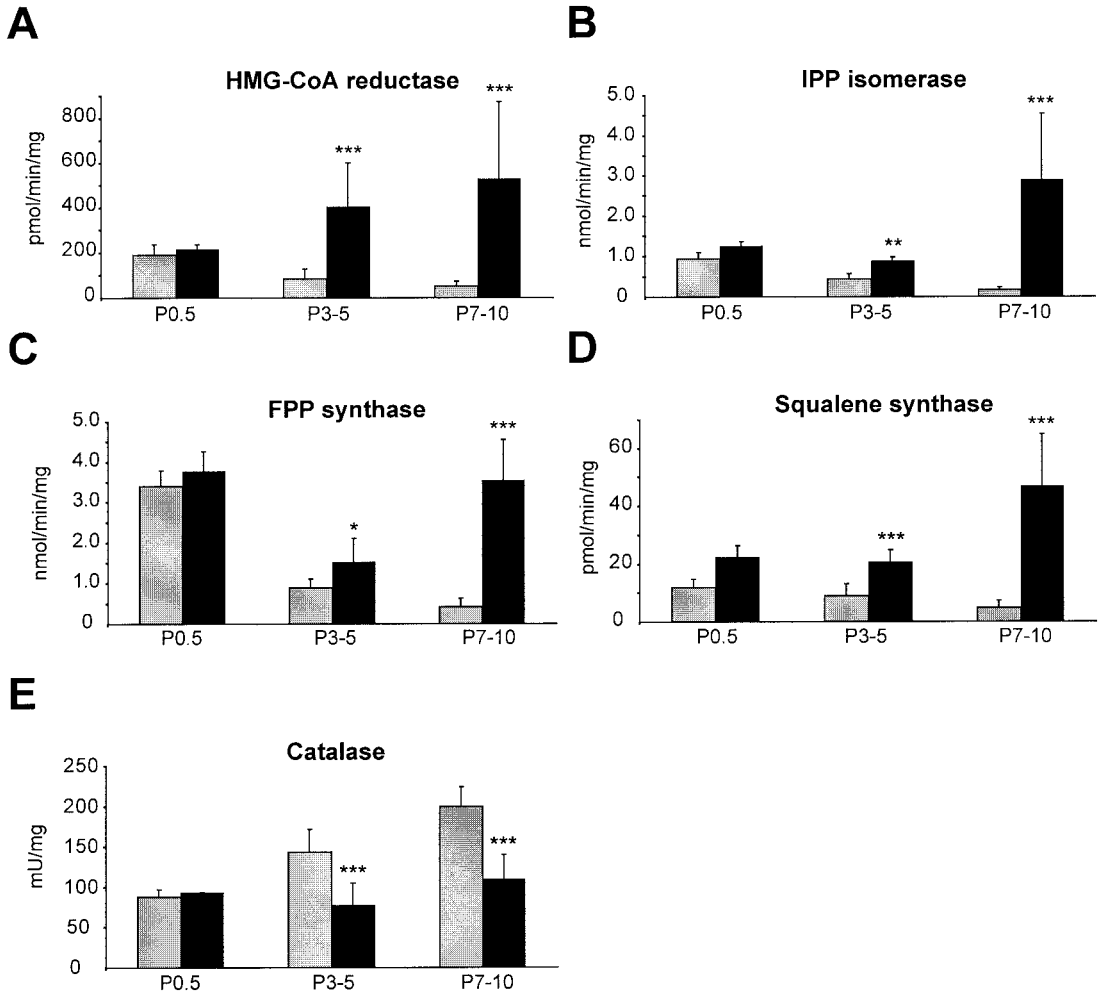

FIG. 1. Activities of selected cholesterol biosynthetic enzymes (A to D) and the peroxisomal marker enzyme catalase (E) in liver homogenates. Since enzyme activities from *PEX2* heterozygous and wild-type mice were similar at the three investigated time points, these data were combined. Data from wild-type and heterozygous (grey bars) and *PEX2*$^{-/-}$ (black bars) mice are shown. Enzyme activities were measured in liver homogenates from mice at three different time points: newborn (P0.5), 3- to 5-day-old (P3–5) and 7- to 10-day-old (P7–10) mice. Values are mean and standard error of the mean ($n = 10$ for wild-type and heterozygous mice; $n = 7$, for *PEX2*$^{-/-}$ mice). *, $P < 0.02$; **, $P < 0.005$; ***, $P < 0.001$ (significant differences between control and *PEX2*$^{-/-}$ mice).

seen with the cholesterol biosynthetic enzyme activities in P7–10 *PEX2*$^{-/-}$ mice (Fig. 1). The protein levels of these cholesterol biosynthetic enzymes in P3–5 *PEX2*$^{-/-}$ mice were also significantly increased compared to those in wild-type and heterozygous mice (data not shown), although the increase was smaller than in P7–10 mice.

Cholesterol biosynthetic gene, SREBP-2, Insig-1, Insig-2, and LDLR mRNA levels are markedly increased in the livers

TABLE 2. Activities of cholesterol biosynthetic enzymes in kidneys and spleen of 10-day-old wild-type, heterozygous, and *PEX2* knockout mice

Enzyme	Enzyme activity (pmol/min/mg of protein) in[a]:			
	Kidneys		Spleen	
	Wild-type mice	*PEX2*$^{-/-}$ mice	Wild-type mice	*PEX2*$^{-/-}$ mice
HMG-CoA reductase	65.0 ± 15.8 (12)	36.1 ± 10.9 (6)*	44.9 ± 8.5 (5)	84.4 ± 16.8 (3)**
IPP isomerase	189.9 ± 32.0 (12)	260.7 ± 129.3 (6)	127.0 ± 17.6 (5)	246.8 ± 43.7 (3)*
FPP synthase	288.7 ± 45.4 (13)	540.0 ± 209.0 (7)*	270.8 ± 38.5 (5)	640.0 ± 130.9 (3)*
Squalene synthase	2.54 ± 1.14 (13)	5.08 ± 2.78 (7)***	ND[b]	ND

[a] Each value represents the mean ± standard error of the mean. Values in parentheses denote the number of samples. Spleens from four *PEX2*$^{-/-}$ mice were pooled and assayed ($n = 3$). Enzyme activities from wild-type and heterozygous mice were similar and were combined. *, $P < 0.001$; **, $P < 0.005$; ***, $P < 0.01$ (Student's *t* test).

[b] ND, not determined.

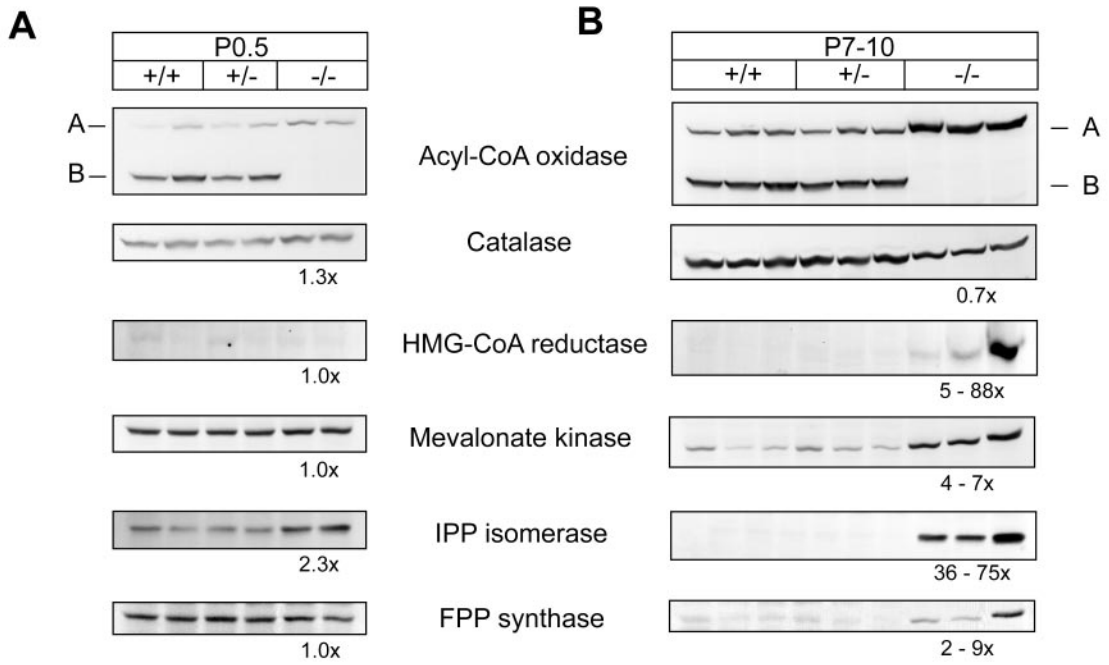

FIG. 2. Immunoblot analysis of 200 μg of liver protein for acyl-CoA oxidase, catalase, and selected cholesterol biosynthetic enzymes in P0.5 (A) and P7–10 (B) wild-type (+/+), heterozygous (+/−), and *PEX2*$^{-/-}$ (−/−) mice. The fold change in the protein level in *PEX2*$^{-/-}$ mice was expressed relative to that in matching wild-type and heterozygous mice, which in each case was arbitrarily set at 1.0. These values are shown below in each blot. The exposure time for the P0.5 and P7–10 immunoblots was the same.

of *PEX2*$^{-/-}$ mice. Next, the mRNA expression levels for a number of cholesterol biosynthetic enzymes were evaluated. Figure 3A shows the relative levels of cholesterol biosynthetic gene mRNAs in the livers of 10-day-old wild-type, heterozygous, and *PEX2*$^{-/-}$ mice. *PEX2*$^{-/-}$ mice exhibited marked increases in the levels of mRNAs encoding cholesterol biosynthetic enzymes (4- to 26-fold). The greatest fold increase was observed for HMG-CoA reductase, IPP isomerase, FPP synthase, and lanosterol synthase (20- to 26-fold). The experiments demonstrate that essentially all the SREBP-2-regulated cholesterol biosynthetic enzymes were markedly increased at the mRNA level in the livers of *PEX2*$^{-/-}$ mice.

SREBP-1 activates the transcription of fatty acid biosynthetic genes, whereas SREBP-2 favors genes in the cholesterol biosynthetic pathway (27). SREBP-2 mRNA levels in *PEX2*$^{-/-}$ mice were elevated by about 2.5-fold (Fig. 3B, right three lanes). In contrast, SREBP-1 mRNA levels were ~85% reduced in *PEX2*$^{-/-}$ mice. Recently, several new membrane-bound proteins (insulin-induced genes 1 and 2 [Insig-1 and Insig-2]) have been identified that bind to the sterol-sensing domain of the SREBP cleavage-activating protein (SCAP) (57, 58). The binding of Insig-1 to SCAP in the presence of cholesterol leads to endoplasmic reticulum retention of the SCAP-SREBP complex. In addition, Insig-1 is itself a target of SREBP gene control whereas Insig-2 is expressed constitutively. Studies suggest that when sterols are limiting, Insig-1 is induced and its product regulates SREBP. Therefore, we estimated the mRNA levels of both Insig-1 and Insig-2. Figure 3B shows an increase of 2.2- to 5.0-fold in Insig-1 and 1.7-fold in Insig-2 mRNA levels in *PEX2*$^{-/-}$ mice.

The mRNA level of the SREBP-regulated LDL receptor was elevated 7.5-fold in the liver of 10-day-old *PEX2*$^{-/-}$ mice (Fig. 3C). The levels of the scavenger receptor BI (SR-BI) mRNAs were the same in the livers of wild-type and *PEX2*$^{-/-}$ mice (data not shown).

Measurement of the rate of in vivo cholesterol synthesis and tissue cholesterol levels. We next explored whether the increased expression, protein levels, and activities of cholesterol biosynthetic enzymes were a consequence of changes in hepatic sterol metabolism (cholesterol content and cholesterol biosynthesis rate). To address this question, mice were injected subcutaneously with [^{3}H]acetate and various tissues (liver, brain, kidneys, heart, lungs, and spleen) were analyzed for sterol content and rate of biosynthesis.

The reverse-phase radio-HPLC chromatograms for nonsaponifiable lipids obtained from livers of 8-day-old wild-type and *PEX2*$^{-/-}$ mice are shown in Fig. 4A. In the *PEX2*$^{-/-}$ mouse liver (right panels), cholesterol was virtually the only sterol detected in appreciable amounts. However, in the wild-type mouse liver, there was a peak of radioactivity (average retention time, 12.47 min) corresponding to squalene, whereas the *PEX2* knockout mouse liver did not show this peak. Cholesterol represented the majority of the total recovered radioactivity, in both wild-type and knockout mouse livers, coincident with the cholesterol mass peak at a retention time of 10.77 min.

Representative reverse-phase HPLC chromatograms obtained from the brains of 8-day-old control and *PEX2*$^{-/-}$ mice are shown in Fig. 4B. The brains of both control and *PEX2*$^{-/-}$ mice took up the [^{3}H]acetate and metabolized it to sterols, with desmosterol and cholesterol being the only sterols detected in appreciable amounts in both cases. In other major

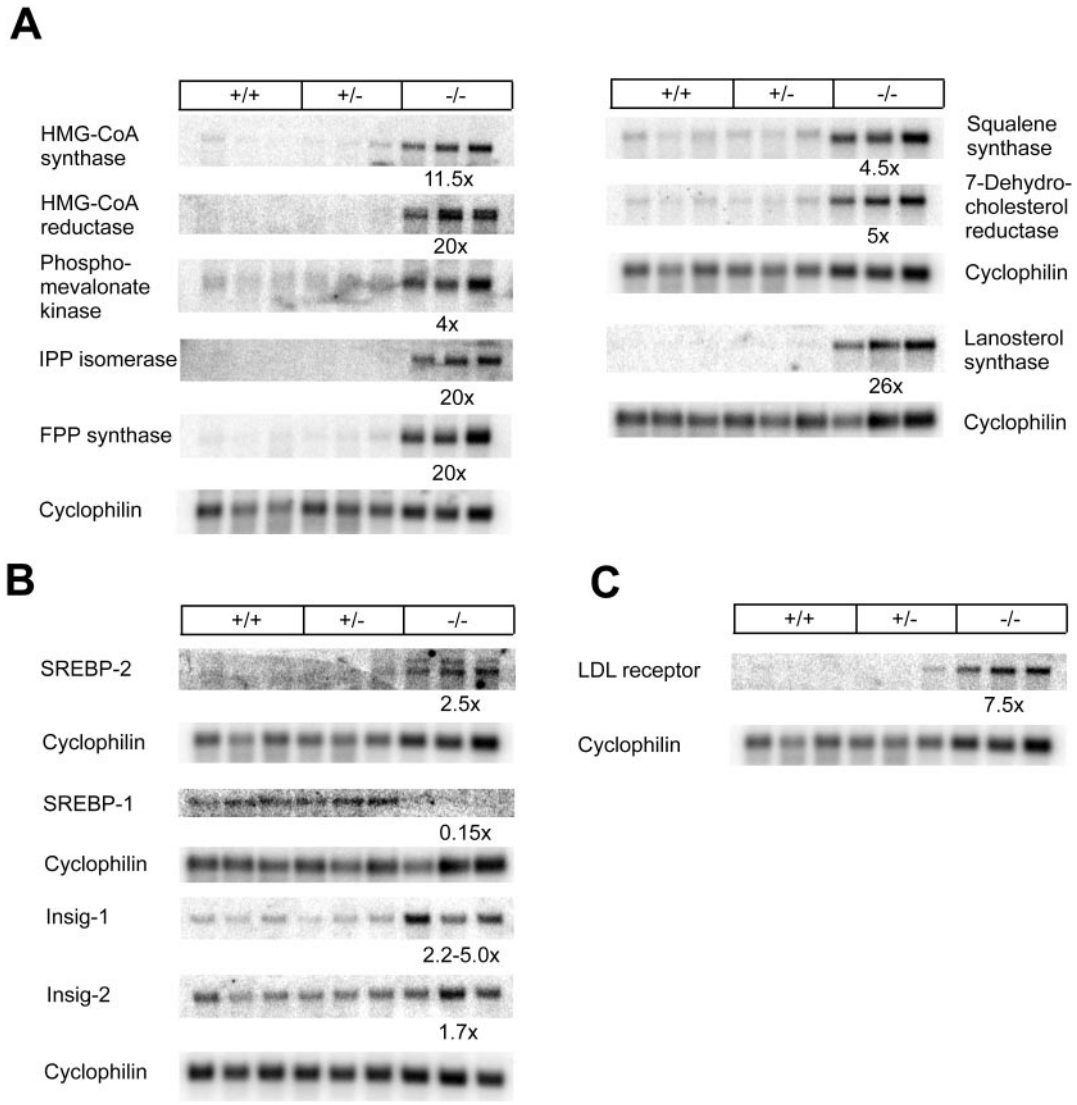

FIG. 3. Northern blot mRNA analysis of cholesterol biosynthetic enzymes (A), SREBPs, Insig-1 and Insig-2 (B), and LDL receptor (C) in the livers of 10-day-old wild-type (+/+), heterozygous (+/−), and *PEX2*$^{-/-}$ (−/−) mice. Aliquots (1.5 μg) of mRNA were subjected to electrophoresis and blot hybridization with the indicated ^{32}P-labeled probe. The amount of radioactivity in each band was quantified by PhosphorImager analysis and normalized to the signal generated by cyclophilin. The fold change in each mRNA of *PEX2*$^{-/-}$ mice was expressed relative to matching wild-type and heterozygous mice, which in each case was arbitrarily set at 1.0. These values are shown below each blot.

PEX2$^{-/-}$ mouse tissues examined (kidneys, spleen, heart, and lungs), cholesterol was the only sterol detected in appreciable amounts, whereas in tissues from wild-type mice there was accumulation of radiolabel in the cholesterol precursors squalene and/or desmosterol (data not shown).

Determination of cholesterol levels in tissues from 10-day-old *PEX2*$^{-/-}$ mice showed that the total cholesterol content in the liver was decreased by ~40% in *PEX2*$^{-/-}$ mice compared with their wild-type or heterozygous littermates (2.36 ± 0.33 mg/g [$n = 9$] and 4.05 ± 0.34 mg/g [$n = 10$], respectively) (Fig. 5A). There was no direct correlation between the weight of the knockout mice (i.e., how well they were thriving) and the level of total cholesterol in the liver. However, in the brain, kidneys, spleen, heart, and lungs, there were no significant differences in total cholesterol levels in *PEX2*$^{-/-}$ and wild-type mice (Fig. 5A). Nonpolar lipid true-mass analysis (Lipomics Technologies Inc., West Sacramento, Calif.) of liver tissue from 10-day-old wild-type and *PEX2*$^{-/-}$ mice confirmed that in the knockout mice the cholesterol ester levels were decreased to ~40% of the control levels (data not shown).

The rate of cholesterol synthesis, expressed as cholesterol specific activity, is shown in Fig. 5B. The specific activity of cholesterol in the livers of 7- to 9-day-old *PEX2*$^{-/-}$ mice was 13-fold higher than in wild-type mice ($P < 0.005$). As shown in the chromatograms (Fig. 4A), wild-type mice show incomplete conversion of [^{3}H]acetate to cholesterol in the liver, with accumulation of radiolabeled squalene and other minor precursors, over the same time interval when *PEX2*$^{-/-}$ mice exhibit nearly quantitative incorporation of [^{3}H]acetate into cholesterol, with little or no appreciable accumulation of radiola-

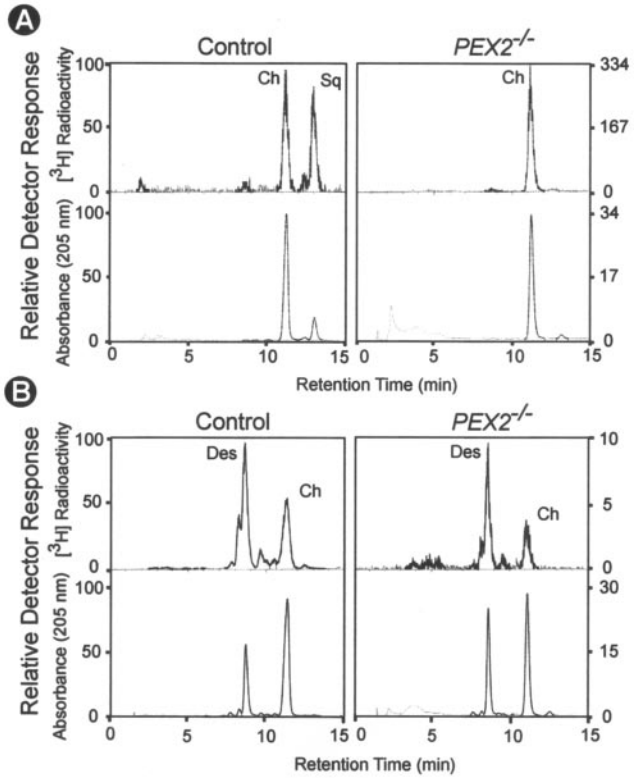

FIG. 4. [^{3}H]acetate incorporation into liver (A) and brain (B) nonsaponifiable lipids. Reverse-phase radio-HPLC chromatograms of nonsaponifiable lipids obtained from 8-day-old control (left) and *PEX2*$^{-/-}$ (right) mouse livers and brains, 6 h after subcutaneous injection with [^{3}H]acetate, are shown. The elution positions for cholesterol (Ch), squalene (Sq), and desmosterol (Des) are indicated. Simultaneous detection was done by scintillation counting (upper panels, total recovered radioactivity: control, 38244 dpm; *PEX2*$^{-/-}$, 102401 dpm) and UV absorbance (at 205 nm, lower panels). The detector response is normalized to the full-scale response for the predominant component, however, the absolute values for controls and *PEX2*$^{-/-}$ mutants are up to 10-fold different.

beled precursors. The squalene content in wild-type mouse livers was 16-fold higher than in *PEX2*$^{-/-}$ mouse livers (39.0 ± 3.0 and 2.5 ± 0.4 μg/g [wet weight], respectively). Consequently, the cholesterol/squalene molar ratio in the livers of *PEX2*$^{-/-}$ mice is 8.5-fold higher than in wild-type mice.

As shown in Fig. 5B, the rate of acetate incorporation into cholesterol in the spleen, lungs, and heart of 7- to 9-day-old *PEX2*$^{-/-}$ mice was significantly increased compared to that in wild-type mice (6-, 2.8- and 4-fold, respectively). However, the rate of incorporation of [^{3}H]acetate into cholesterol is decreased in the brain and kidneys of *PEX2*$^{-/-}$ mice compared to that in wild-type mice. In the brain and kidneys of the knockouts, the specific activity of cholesterol was 2.4-fold ($P < 0.001$) and 2-fold ($P < 0.005$) lower, respectively, than in the controls. Surprisingly, the incorporation of [^{3}H]acetate into a component with the chromatographic properties of desmosterol was much higher than into cholesterol, in both wild-type and *PEX2*$^{-/-}$ mouse brains. However, the specific activities both of desmosterol and cholesterol were lower in the brains of *PEX2*$^{-/-}$ mice than in those of wild-type mice.

Expression of bile acid biosynthetic genes and cholesterol absorption. Our results demonstrate that despite the upregulation of the SREBP-2 pathway and the increased rate of cholesterol biosynthesis in the peroxisome-deficient mouse liver, the cholesterol content is still markedly reduced. Since the balance between de novo cholesterol biosynthesis and catabolism of cholesterol to bile acids is a tightly regulated process in the liver, we investigated the expression levels of the rate-limiting enzymes in bile acid biosynthesis. Cholesterol 7α-hydroxylase (CYP7A1) is the rate-limiting step in the classic pathway of bile acid biosynthesis, and its expression levels were decreased in 10-day-old *PEX2*$^{-/-}$ mice compared to those in wild-type and heterozygous mice (Fig. 6A). Sterol 27-hydroxylase (CYP27A1) initiates the alternate or acidic pathway of bile acid biosynthesis and is also involved in the classic pathway to facilitate the oxidation of the steroid side chain (7, 46). As shown in Fig. 6A, the *PEX2*$^{-/-}$ mice manifest a 2.7-fold increase in the mRNA for sterol 27-hydroxylase in the liver. Oxysterol 7α-hydroxylase (CYP7B1), also an enzyme of the alternate bile acid synthesis pathway which hydroxylates oxysterols at the 7-position (48), was expressed in the livers of P7–10 mice at very low levels and the mRNA level was increased around twofold in mutant mice (data not shown).

These data are in agreement with preliminary studies which demonstrate marked reductions in the concentration of plasma taurocholic acid and increased concentrations of plasma C_{27} bile acids, 3α,7α-dihydroxy-5β-cholestanoic acid (DHCA), produced by the alternate or acidic pathway of bile acid biosynthesis, in *PEX2*$^{-/-}$ mice (M. Duran, R. J. A. Wanders, and P. Faust, unpublished data).

Fecal neutral sterol excretion and the level of intestinal cholesterol absorption are inversely correlated (43, 44, 49). A deficiency of primary bile acids would lead to a diminished level of cholesterol absorption, which would be reflected in a greater loss of sterol in the feces and could contribute to a negative cholesterol balance in the knockout mice. However, the content of cholesterol in stool samples was significantly reduced in the *PEX2*$^{-/-}$ mice. The stool cholesterol content was 11.48 ± 5.31 mg/g ($n = 6$) in the wild-type mice versus 6.64 ± 2.32 mg/g ($n = 7$) in the *PEX2*$^{-/-}$ mice (Fig. 6C). These data would suggest that intestinal cholesterol absorption is not impaired in the *PEX2*$^{-/-}$ mice.

Expression of hepatic nuclear hormone receptors, apolipoproteins, and ABC transporter genes. Recently it has been shown that nuclear hormone receptors, including the liver X-activated receptors (LXRα and LXRβ; NR1H3 and NR1H2), the farnesoid X-activated receptor (FXR; NR1H4), and the pregnane X receptor (PXR; NR112), regulate the expression of genes controlling cholesterol, bile acid, lipoprotein, and drug metabolism (10, 15).

It has been suggested that LXR functions as a sensor of cellular oxysterols and 27-hydroxycholesterol, generated by the activity of sterol 27-hydroxylase (19). Since LXRα is most highly expressed in the liver and the LXRα gene is itself a target of the LXR signaling pathway, we analyzed the expression of LXRα in the livers of 10-day-old mice. No change in the expression of LXRα was observed in peroxisome-deficient mice (Fig. 6A). FXR was also highly expressed in the liver, where it appeared to function as a bile acid sensor. There was

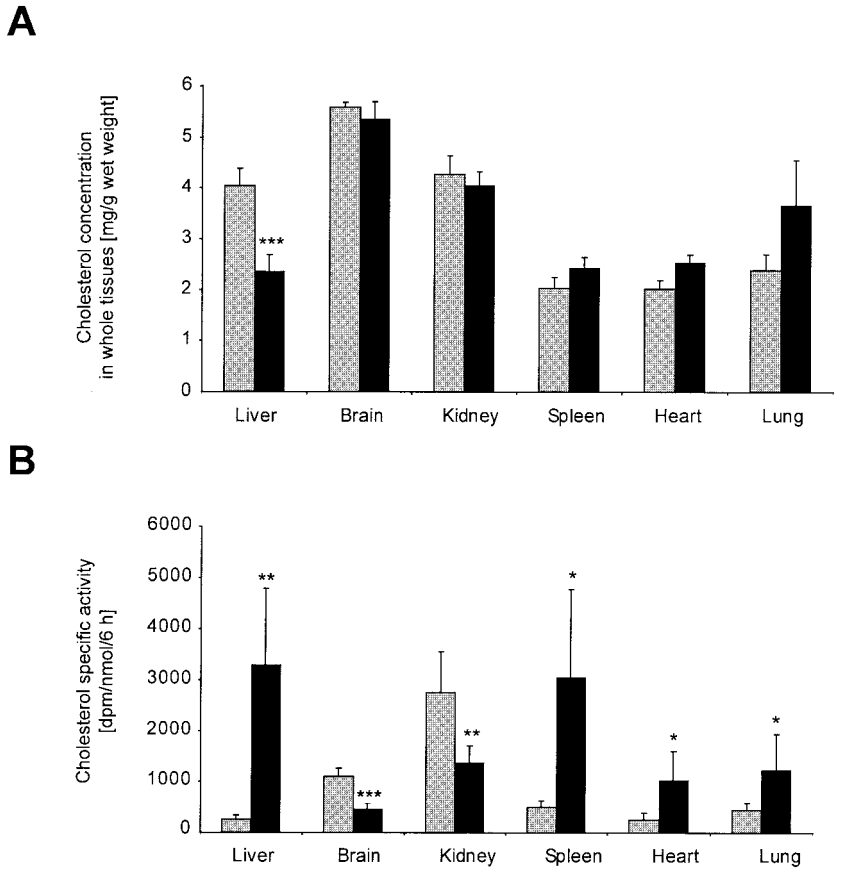

FIG. 5. Cholesterol concentration (A) and rate of cholesterol synthesis (B) in various tissues of wild-type and *PEX2*$^{-/-}$ mice. [^{3}H]acetate was administered to 7- to 9-day-old mice by subcutaneous injection, and the animals were killed 6 h later. The amount of [^{3}H]acetate incorporated into cholesterol in the indicated tissues was determined as described in Materials and Methods. Values represent the mean and standard error of the mean ($n = 5$ for wild-type mice; $n = 6$ for *PEX2*$^{-/-}$ mice). The asterisks show that the value for the *PEX2*$^{-/-}$ animals (black bars) was significantly different from that for the wild-type animals (grey bars). *, $P < 0.05$; **, $P < 0.005$; ***, $P < 0.001$.

no difference in the expression of FXR between wild-type and knockout mice (data not shown).

PXR is activated by elevated intracellular concentrations of toxic bile acids (bile acid intermediates) (9, 20, 51, 56). It regulates a number of target genes encoding proteins with relevance to bile acid metabolism, for example, CYP3A, an enzyme which functions in the detoxification of toxic bile acids. As illustrated in Fig. 6B, steady-state levels of CYP3A11 mRNA, which reflect the activity of PXR, were reduced by 50% ($P < 0.05$) in the livers of 10-day-old *PEX2*$^{-/-}$ mice compared to wild-type and heterozygous mice.

The ABCA and ABCG subclasses of mammalian ABC transporters have been implicated in the cellular homeostasis of phospholipids and cholesterol. ABCA1 controls the rate-limiting step in cellular phospholipid and cholesterol efflux (38), and hepatic expression of the ABCA1 transporter appears to be critical in controlling plasma HDL cholesterol levels (3). ABCG1 may also play a role in cholesterol efflux, although its role is not well defined (29). The expression of ABCA1 and ABCG1 in the livers of 10-day-old wild-type, heterozygous, and *PEX2*$^{-/-}$ mice was evaluated by Northern blot analysis and found to be unchanged (Fig. 6A). However, the hepatic expression of apoA-1, the major apolipoprotein of HDL, and apoC-III was significantly reduced in the *PEX2*$^{-/-}$ mice compared to the control mice, suggesting that the synthesis of nascent HDL is decreased in peroxisome-deficient mice (Fig. 6B).

Lastly, we determined the hepatic expression of ABCG5 and ABCG8, two ABC half-transporters that work cooperatively and have been proposed to play a key role in the biliary excretion of sterols (22, 59). In the liver, the *ABCG5* and *ABCG8* genes are direct targets of the nuclear receptor LXR. Surprisingly, in the livers of 10-day-old *PEX2*$^{-/-}$ mice, the expression of ABCG5 was decreased whereas the expression of ABCG8 was increased compared to that in wild-type mice (Fig. 6A), indicating a loss of coordinate regulation of ABCG5 and ABCG8 in *PEX2*$^{-/-}$ mice. The lack of upregulation of the LXR target genes *Cyp7a1*, *ABCA1*, *ABCG1*, and *LXR* in *PEX2*$^{-/-}$ mice suggests that the LXR pathway is not activated in *PEX2*$^{-/-}$ mice. Furthermore, there was no change in the expression of FXR, and the levels of CYP3A11 mRNA, which reflect the activity of PXR, were reduced, indicating a lack of activation of these two pathways as well.

Altered catalytic efficiency of cholesterol biosynthetic enzymes. Since peroxisomal deficiency results in mislocalization of peroxisomal matrix enzymes to the cytosol, we asked

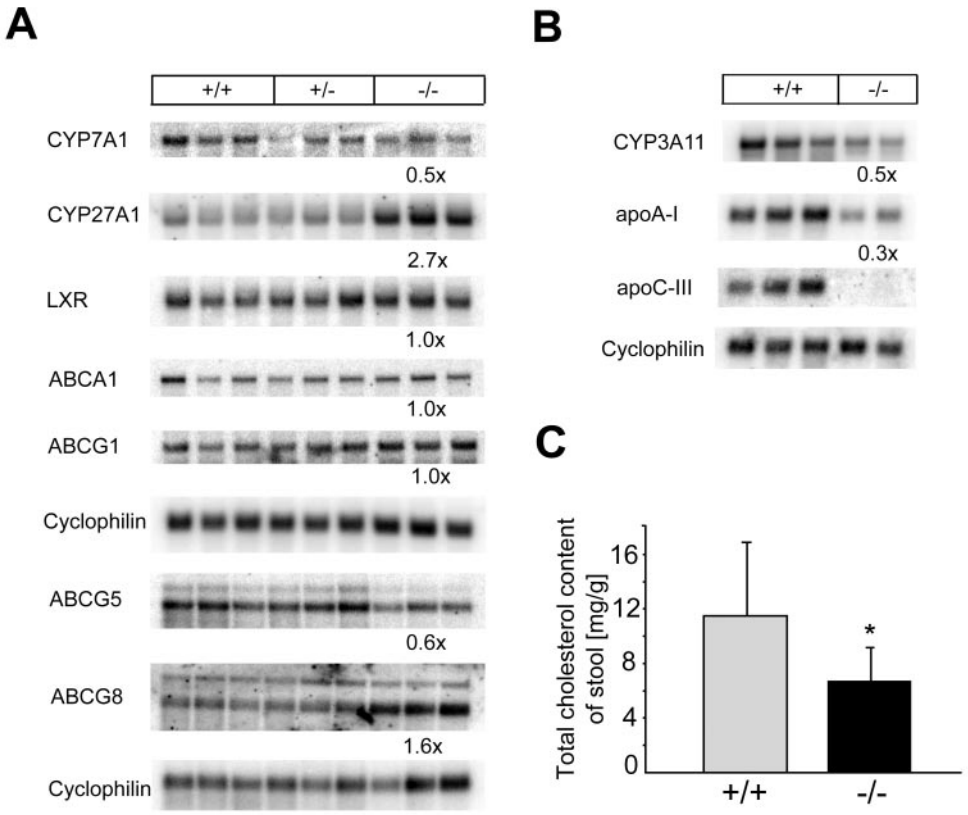

FIG. 6. (A and B) Northern blot mRNA analysis of bile acid biosynthetic genes (*Cyp7a1*, *Cyp27a1*), proteins involved in sterol transport (ABC transporters), nuclear hormone receptor LXR, apolipoproteins, and *Cyp3a11*. Aliquots (4 μg) of mRNA were subjected to electrophoresis and blot hybridization with the indicated ^{32}P-labeled probe. The amount of radioactivity in each band was quantified by PhosphorImager analysis and normalized to the signal generated by cyclophilin. The fold change in each mRNA of *PEX2*$^{-/-}$ mice was expressed relative to matching wild-type and heterozygous mice, which in each case was arbitrarily set at 1.0. These values are shown below each blot. (C) Stool cholesterol content in wild-type (+/+) and *PEX2* knockout (−/−) mice. The stools of neonatal animals were collected from suckling wild-type and knockout mice, and cholesterol was determined by reverse-phase HPLC after saponification and petroleum ether extraction. Values represent the mean and standard error of the mean ($n = 6$ for wild-type mice; $n = 7$ for *PEX2*$^{-/-}$ mice). The asterisk shows that the value for the *PEX2*$^{-/-}$ animals (black bars) was significantly different from that for the wild-type animals (grey bars) ($P = 0.05$).

whether the cholesterol biosynthetic enzymes in the *PEX2*$^{-/-}$ mice have the same catalytic specific activity in the cytoplasm as in peroxisomes. Since measurements of enzyme activities and immunoblots were done on the same liver samples, we were able to normalize the specific activities to the enzyme protein content. Table 3 shows the specific activity of HMG-CoA reductase normalized to the HMG-CoA reductase protein content in the livers of 10-day-old control and knockout mice. The specific activity of HMG-CoA reductase was reduced by 55% ($P < 0.01$) in *PEX2*$^{-/-}$ mice when normalized to the HMG-CoA reductase protein content in the liver. The same type of calculation was performed for IPP isomerase and FPP synthase, enzymes that are located predominantly in peroxisomes. Whereas the specific activity of IPP isomerase in the *PEX2*$^{-/-}$ mice was decreased by 70% ($P < 0.001$), the specific activity of FPP synthase was increased 3.3-fold ($P < 0.05$) in the knockout mice when normalized to the protein level. Similar trends in altered specific activity were observed for the other time points, P0 and P3–5 mice (data not shown). These data, illustrating that mislocalization of peroxisomal cholesterol biosynthetic enzymes to the cytoplasm alters the normal catalytic efficiency of these enzymes, support our conjecture that the compartmentalization of cholesterol biosynthetic enzymes may be an important regulatory mechanism for cholesterol biosynthesis.

DISCUSSION

The effects of inactivation of the mouse *PEX2* gene which results in peroxisomal deficiency were evaluated in regards to sterol homeostasis. The major finding of this study is that inactivation of the *PEX2* gene results in a reduction of the steady-state concentration of cholesterol in the livers of *PEX2*$^{-/-}$ mice by at least 40% and in reduced levels of plasma total cholesterol and HDL cholesterol. Despite the activation of a number of regulatory pathways and an increased rate of hepatic cholesterol de novo synthesis, normal cholesterol homeostasis was not achieved in the *PEX2*$^{-/-}$ mice, denoting the necessity of functional peroxisomes for this process.

SREBP-2-induced cholesterol biosynthetic pathway enzymes function with altered efficiency in *PEX2*$^{-/-}$ mice. Mammalian cells keep their cholesterol content under tight

TABLE 3. Specific activity of HMG-CoA reductase normalized to HMG-CoA reductase protein content in the livers of 10-day-old wild-type, heterozygous, and *PEX2* knockout mice[a]

Genotype	Sp act (pmol/min/mg)	Vol density (per mg of protein)	Sp act/vol density (fmol/min)	Avg sp act/vol density[b]
+/+	60	216	278	291.2 ± 70.7 (100%)
+/+	34	83	410	
+/+	58	173	335	
+/−	45	209	215	
+/−	38	157	242	
+/−	51	191	267	
−/−	141	876	163	132.7 ± 26.8* (45%)
−/−	258	2,300	112	
−/−	1,851	15,109	123	

[a] Measurements of HMG-CoA reductase activities and immunoblots were done on the same liver samples. For Western blot analysis, 200 μg of protein was separated on an SDS–7.5% polyacrylamide gel, transferred to a nitrocellulose membrane, and subjected to immunoblot analysis using a polyclonal anti-(HMG-CoA reductase) antibody.

[b] *, $P < 0.01$ (Student's t test).

transcriptional control by the actions of a family of membrane-bound transcription factors, the SREBPs (27). In vivo, SREBP-2 preferentially activates genes of cholesterol metabolism whereas SREBP-1c preferentially activates genes of fatty acid and triglyceride metabolism. Depletion of hepatic cholesterol elicited the expected increase in the processing of SREBP-2 in the livers of *PEX2*$^{-/-}$ mice. The transcription of the SREBP-1c gene decreased, perhaps owing to a deficiency of an endogenous oxysterol ligand for the liver X receptor, which is required for SREBP-1c production (8, 42). In the present study, we demonstrated SREBP-2 activation of various enzymes in the cholesterol biosynthetic pathway in the liver of *PEX2*$^{-/-}$ mice: HMG-CoA synthase, HMG-CoA reductase, phosphomevalonate kinase, IPP isomerase, FPP synthase, squalene synthase, lanosterol synthase, and 7-dehydrocholesterol reductase. All these cholesterogenic genes have sterol regulatory element (SRE)-like sequences and are well-established SREBP target genes (27). The determination of enzyme activities and protein levels of these cholesterol biosynthetic enzymes also showed that in the livers of *PEX2*$^{-/-}$ mice, both activities and protein levels are highly increased.

The benefit of the compartmentalization of the cholesterol biosynthetic enzymes in peroxisomes is still not clear, but it may ensure optimal cofactor concentrations for the individual reactions, keep enzymes together in operating units, or perhaps provide additional regulatory mechanisms for cholesterol biosynthesis. Since the mislocalized cholesterol biosynthetic enzymes in the *PEX2*$^{-/-}$ mice appear to be stable in the cytoplasm, we asked whether the enzymes are also as efficient in the cytoplasm as they are in peroxisomes. Unexpectedly, the specific activity of HMG-CoA reductase was reduced by 55% in *PEX2*$^{-/-}$ mice when normalized to the HMG-CoA reductase protein content in liver (Table 3). The decreased specific activity of HMG-CoA reductase is very surprising, since this enzyme is localized in both the endoplasmic reticulum and peroxisomes, with the major portion being mainly in the endoplasmic reticulum. We did the same calculation for IPP isomerase and FPP synthase, enzymes that are localized predominantly in peroxisomes. Whereas the specific activity of IPP isomerase in the *PEX2*$^{-/-}$ mice was decreased by 70%, the specific activity of FPP synthase was increased 3.3-fold in mutant mice when normalized to the protein level. Clearly, mislocalization of these enzymes to the cytoplasm alters the normal catalytic efficiency. The change in the catalytic efficiency of the enzymes may also explain the differences observed in the levels of sterol intermediates between the control and knockout mice (accumulation of squalene in the livers of wild-type animals but not in the *PEX2*$^{-/-}$ mice).

SREBP-2 pathway induction in *PEX2*$^{-/-}$ mice increases in the postnatal period. Both newborn (data not shown) and postnatal *PEX2*$^{-/-}$ mice have reduced total cholesterol levels in plasma. While the activities and protein levels for most of the cholesterol biosynthetic enzymes are not markedly increased in newborn mutant mice (Fig. 1 and 2), normalization of enzyme activity to enzyme protein level suggests that abnormalities in the functioning of these enzymes also exist in the newborn *PEX2*$^{-/-}$ liver. However, it is clear that the induction of cholesterol enzymes by SREBP-2 pathway activation is exacerbated in the postnatal period in *PEX2*$^{-/-}$ mice. This postnatal exacerbation may reflect, at least in part, the significant liver disease that develops in knockout mice, with onset of hepatic steatosis and marked intrahepatic cholestasis (P. Faust, unpublished data). *PEX2*$^{-/-}$ mice also have bulky, yellow stools, which is suggestive of a malabsorption syndrome due to the defective bile acid synthesis. Thus, malnutrition in *PEX2*$^{-/-}$ mice may also further hinder the functioning of the liver.

Interestingly, studies with *PEX5*$^{-/-}$ mice have demonstrated the presence of severe hepatic mitochondrial abnormalities which were postulated to be associated with oxidative damage due to peroxisome deficiency (5). We have observed similar mitochondrial changes in newborn *PEX2*$^{-/-}$ mice and are currently investigating whether this damage is exacerbated in the postnatal mutant liver. Thus, the continually increased induction of peroxisomal enzymes in the absence of proper cellular compartmentalization may lead to accumulation of abnormal metabolites in the cytosol and secondary organellar dysfunction. The decreased specific activity of HMG-CoA reductase (when normalized to HMG-CoA protein levels [Table 3]) observed in the *PEX2*$^{-/-}$ mouse liver raises the possibility that there is a functional abnormality in the endoplasmic reticulum which is not readily observable at a morphologic level.

***PEX2*$^{-/-}$ mice are unable to maintain normal cholesterol homeostasis.** The fetus derives cholesterol mainly from de novo synthesis, and the rates of sterol synthesis are much higher in the fetus than in the adult when expressed on a per-gram-of-tissue basis (55). Hepatic cholesterol synthesis continues in the period immediately following birth but then declines as suckling becomes established (24). These studies are in agreement with our findings that activities and protein levels of cholesterol biosynthetic enzymes in the liver of newborn wild-type mice are much higher than in P3–5 and P7–10 mice. However, in the livers of *PEX2*$^{-/-}$ mice the activities and protein levels of cholesterol biosynthetic enzymes did not decline but increased significantly during postnatal development, indicating an increased need for de novo cholesterol biosynthesis.

In the mouse, ~70% of the cholesterol demand is met through de novo synthesis and 30% is met through absorption

(39). Fecal neutral sterol excretion and the level of intestinal cholesterol absorption are normally inversely correlated. Recently, Repa et al. (44) reported that feeding of SCH 58053, a selective cholesterol absorption inhibitor, to 13- to 20-week-old mice resulted in reduced intestinal cholesterol absorption, an increased rate of fecal neutral sterol excretion, a 2.9-fold increase in hepatic sterol synthesis, and no change in the rate of cholesterol synthesized by extrahepatic tissues. In our study, we observed a significantly greater increase in hepatic cholesterol synthesis (13-fold) and increased rates of cholesterol synthesis in most peripheral organs of 7- to 9-day-old *PEX2*$^{-/-}$ mice, with the exception of the brain and kidneys, where the rates were decreased. Thus, the pattern and extent of the cholesterol synthesis alterations in *PEX2*$^{-/-}$ mice differ significantly from that induced by intestinal cholesterol loss. In addition, while one might expect that a deficiency of bile acids in *PEX2*$^{-/-}$ mice would lead to a diminished level of intestinal cholesterol absorption, the content of cholesterol in stool samples was significantly reduced in the *PEX2*$^{-/-}$ mice (Fig. 6C). These data indicate that intestinal cholesterol absorption is not significantly impaired in the *PEX2*$^{-/-}$ mice and that fecal loss does not contribute to the negative cholesterol balance in these mutant mice.

Studies with mice deficient in cholesterol 7α-hydroxylase (*Cyp7a1*$^{-/-}$ mice) have shown that this enzyme is essential for proper absorption of dietary lipids and fat-soluble vitamins in newborn mice but not for the maintenance of serum or hepatic cholesterol levels (28, 47). The serum cholesterol content was similar in wild-type and *Cyp7a1*$^{-/-}$ mice and in sterol 27-hydroxylase knockout (*Cyp27a1*$^{-/-}$) mice (43, 47, 49). Furthermore, the concentration of cholesterol in several tissues (liver, kidneys, spleen, lungs, and heart) was normal in 15-day-old *Cyp7a1*$^{-/-}$ mice and the rate of cholesterol biosynthesis was increased in the *Cyp7a1*$^{-/-}$ mouse liver. In these mutant mice, the response of the homeostatic regulatory mechanisms was sufficient to maintain serum lipid and cholesterol levels even when key bile acid catabolic pathways were knocked out. With respect to these data, a deficiency or reduced levels of primary bile acids and a concomitant malabsorption of dietary lipids is not sufficient to explain the disturbed cholesterol homeostasis we observed in the *PEX2*$^{-/-}$ mouse.

Diversity of cholesterol homeostatic responses in *PEX2*$^{-/-}$ mice. Our studies also demonstrate that the cholesterol homeostatic response to peroxisome deficiency differs in various organs. In most tissues, such as the liver, spleen, lungs, and heart, the synthesis rate of cholesterol is increased. The brain and kidneys displayed normal cholesterol levels but were the only two tissues that showed a decreased rate of cholesterol synthesis. In the knockout mouse kidneys, the HMG-CoA reductase activity was also decreased, in agreement with the synthesis data. Thus, different regulatory mechanisms for maintaining cholesterol levels clearly exist in the kidneys. Catabolism of cholesterol by cholesterol 24-hydroxylase (*CYP46a1*) is postulated to be the major tissue-specific pathway for cholesterol turnover in the brain. Interestingly, a recent study of *Cyp46a1*$^{-/-}$ mice reported a 40% reduction in de novo cholesterol biosynthesis in the brain, despite the steady-state levels of cholesterol being similar in the knockout mice (32). Future studies will analyze the levels of cholesterol biosynthetic enzymes and the regulation of central nervous system cholesterol turnover in different parts of the *PEX2*$^{-/-}$ mouse brain.

Altered bile acid pathway regulation in *PEX2*$^{-/-}$ mice. It is well established that chain shortening of the methyl-branched side chain of the bile acid intermediates DHCA and 3α,7α,12α-trihydroxy-5β-cholestanoic acid (THCA) takes place in peroxisomes (41), resulting in the formation of the primary bile acids (chenodeoxycholic and cholic acid, respectively). Since the liver plays a central role in maintaining whole-body cholesterol homeostasis and is the site of bile acid synthesis, we investigated whether altered bile acid pathway metabolism may contribute to the inability of *PEX2*$^{-/-}$ mice to maintain hepatic and plasma cholesterol levels. Bile acids are synthesized via the classic pathway, initiated by cholesterol 7α-hydroxylase (CYP7A1), or via the alternate pathway, which utilizes sterol 27-hydroxylase (CYP27A1) as the rate-limiting enzyme and a different sequence of initial steps (45). In this study we unexpectedly observed decreased expression levels of CYP7A1 and increased expression of CYP27A1 in *PEX2*$^{-/-}$ mice.

As CYP7A1 is normally feedback downregulated by bile acids (45), one might expect this enzyme to be upregulated in *PEX2*$^{-/-}$ mice as a result of the paucity of primary bile acids. However, the downregulation of CYP7A1 would tend to preserve cellular cholesterol levels in the mutant mouse liver, which may be a dominating force. The regulation of CYP7A1 is highly complex, with multiple nuclear hormone receptor pathways having both positive and negative effects, along with non-receptor-mediated cytokine repression (35, 45). The function of the CYP27A1 gene upregulation in *PEX2*$^{-/-}$ mice is not understood but may provide a pathway for some primary bile acid synthesis in the presence of CYP7A1 downregulation. It is possible that activation of the CYP27A1 pathway, along with upregulation of CYP7B1 (data not shown), results in hepatic loss of cholesterol and inability of the increased synthesis rate to maintain normal cholesterol levels in the mutant mouse liver. Interestingly, several of the endogenous bile acid precursors identified as ligands for PXR activation occur upstream of CYP27A1 activity (20). The lack of PXR pathway activation in *PEX2*$^{-/-}$ mice, as indicated by the reduced CYP3A11 gene expression (Fig. 6B), indicates that the level of these intermediates is probably lower in the knockout mouse liver due to the increased 27-hydroxylase expression. Additional studies are necessary to further document the bile acid abnormalities and complex regulatory pathways in *PEX2*$^{-/-}$ mice.

In summary, the present study shows that the deficiency of peroxisomes as a result of the *PEX2* knockout leads to an incapacity to maintain normal hepatic and plasma cholesterol levels, suggesting a loss of coordinate regulation for cholesterol homeostasis. This finding is contrary to results obtained with other mouse models which have deletions of major pathways involved in cholesterol regulation (*Cyp7a1* and *Cyp27a1* knockout mice) yet are able to maintain normal hepatic and plasma cholesterol levels. Future studies will focus on an analysis of bile acids and on deducing the complex regulatory pathways for cholesterol homeostasis in various organs in the *PEX2*$^{-/-}$ mice.

ACKNOWLEDGMENTS

This work was supported by National Institutes of Health (NIH) grants DK58238 and DK58040 to S.K.K., by NIH grant EY07361 to S.J.F., by a Max Kade Postdoctoral Exchange grant to W.J.K, and by NIH grant HD36807 to P.L.F. S.J.F. received additional support, in part, from an unrestricted departmental grant from Research to Prevent Blindness and from The Norman J. Stupp Foundation.

We thank Vardiella Meiner for the mouse CYP27A1 cDNA; David Russell for the mouse CYP7B1 cDNA; Herbert Stangl for cDNAs for apoA-I, apoC-III, and SR-BI; Roger Davis for the CYP7A1 cDNA; Peter Edwards for the HMG-CoA synthase cDNA; Timothy Osborne for the SREBP cDNAs; and Helen Hobbs for the mouse ABCG5 and ABCG8 cDNAs. We thank Herbert Stangl and Roger Davis for helpful discussions.

REFERENCES

1. **Aboushadi, N., and S. K. Krisans.** 1998. Analysis of isoprenoid biosynthesis in peroxisomal-deficient Pex2 CHO cell lines. J. Lipid Res. **39:**1781–1791.
2. **Baes, M., P. Gressens, E. Baumgart, P. Carmeliet, M. Casteels, M. Fransen, P. Evrard, D. Fahimi, P.E. Declercq, D. Collen, P.P. van Veldhoven, and G.P. Mannaerts.** 1997. A mouse model for Zellweger syndrome. Nat. Genet. **17:**49–57.
3. **Basso, F., L. Freeman, C.L. Knapper, A. Remaley, J. Stonik, E.B. Neufeld, T. Tansey, M.J.A. Amar, J. Fruchart-Najib, N. Duverger, S. Santamarina-Fojo, and H.B. Brewer.** 2003. Role of the hepatic ABCA1 transporter in modulating intrahepatic cholesterol and plasma HDL cholesterol concentrations. J. Lipid Res. **44:**296–302.
4. **Baudhuin, P., H. Beaufay, Y. Rahman-Li, O. Z. Sellinger, R. Wattiaux, P. Jacques, and C. De Duve.** 1964. Tissue fractionation studies. Intracellular distribution of monoamine oxidase, aspartate aminotransferase, alanine aminotransferase, D-amino acid oxidase and catalase in rat liver tissue. Biochem. J. **92:**179–184.
5. **Baumgart, E., I. Vanhorebeek, M. Grabenbauer, M. Borgers, P. E. Declercq, H. D. Fahimi, and M. Baes.** 2001. Mitochondrial alterations caused by defective peroxisomal biogenesis in a mouse model for Zellweger syndrome (*PEX5* knockout mouse). Am. J. Pathol. **159:**1477–1494.
6. **Biardi, L., A. Sreedhar, A. Zokaei, N. B. Vartak, R. L. Bozeat, J. E. Shackelford, G. A. Keller, and S. K. Krisans.** 1994. Mevalonate kinase is predominantly localized in peroxisomes and is defective in patients with peroxisome deficiency disorders. J. Biol. Chem. **269:**1197–1205.
7. **Björkhem, I.** 1992. Mechanism of degradation of the steroid side chain in the formation of bile acids. J. Lipid Res. **33:**455–471.
8. **DeBose-Boyd, R. A., J. Ou, J. L. Goldstein, and M. S. Brown.** 2001. Expression of sterol regulatory element-binding protein 1c (SREBP-1c) mRNA in rat hepatoma cells requires endogenous LXR ligands. Proc. Natl. Acad. Sci. USA **98:**1477–1482.
9. **Dussault, I., H. D. Yoo, M. Lin, E. Wang, M. Fan, A. K. Batta, G. Salen, S. K. Erickson, and B. M. Forman.** 2003. Identification of an endogenous ligand that activates pregnane X receptor-mediated sterol clearance. Proc. Natl. Acad. Sci. USA **100:**833–838.
10. **Edwards, P. A., H. R. Kast, and A. M. Anisfeld.** 2002. BAREing it all: the adoption of LXR and FXR and their roles in lipid homeostasis. J. Lipid Res. **43:**2–12.
11. **Engfelt, W. H., J. E. Shackelford, N. Aboushadi, N. Jessani, K. Masuda, V. G. Paton, G. A. Keller, and S. K. Krisans.** 1997. Characterization of UT2 cells. J. Biol. Chem. **272:**24579–24587.
12. **Faust, P. L.** 2003. Abnormal cerebellar histogenesis in *PEX2* Zellweger mice reflects multiple neuronal defects induced by peroxisome deficiency. J. Comp. Neurol. **461:**394–413.
13. **Faust, P. L., and M. E. Hatten.** 1997. Targeted deletion of PEX2 peroxisome assembly gene in mice provides a model for Zellweger syndrome, a human neuronal migration disorder. J. Cell Biol. **139:**1293–1305.
14. **Faust, P. L., H.-M. Su, A. Moser, and H. W. Moser.** 2001. The peroxisome deficient PEX2 Zellweger mouse. J. Mol. Neurosci. **16:**289–297.
15. **Fitzgerald, M. L., K. J. Moore, and M. W. Freeman.** 2002. Nuclear hormone receptors and cholesterol trafficking: the orphans find a new home. J. Mol. Med. **80:**271–281.
16. **Fliesler, S. J., M. J. Richards, C.-Y. Miller, and R. J. Cenedella.** 2000. Cholesterol synthesis in the vertebrate retina: effects of U18666A on rat retinal structure, photoreceptor membrane assembly, and sterol metabolism and composition. Lipids **35:**289–296.
17. **Fliesler, S. J., M. J. Richards, C.-Y. Miller, and N. S. Peachey.** 1999. Marked alteration of sterol metabolism and composition without compromising retinal development or function. Investig Ophthalmol. Visual Sci. **40:**1792–1801.
18. **Friedewald, W. T., R. J. Levy, and D. S. Fredrickson.** 1972. Estimation of the concentration of low-density-lipoprotein cholesterol in plasma without use of the preparative ultracentrifuge. Clin. Chem. **18:**499–502.
19. **Fu, X., J. G. Menke, Y. Chen, G. Zhou, K. L. MacNaul, S. D. Wright, C. P. Sparrow, and E. G. Lund.** 2001. 27-Hydroxycholesterol is an endogenous ligand for liver X receptor in cholesterol-loaded cells. J. Biol. Chem. **276:**38378–38387.
20. **Goodwin, B., K. C. Gauthier, M. Umetani, M. A. Watson, M. I. Lochansky, J. L. Collins, E. Leitersdorf, D. J. Mangelsdorf, S. A. Kliewer, and J. J. Repa.** 2003. Identification of bile acid precursors as endogenous ligands for the nuclear xenobiotic pregnane X receptor. Proc. Natl. Acad. Sci. USA **100:**223–228.
21. **Gould, S. J., D. Valle, and G. V. Raymond.** 2001. The peroxisome biogenesis disorders, p. 3181–3217. *In* C. R. Scriver, A. L. Beaudet, W. S. Sly, and D. Valle (ed.), The metabolic and molecular bases of inherited disease, 8th ed., vol. 2. McGraw-Hill Book Co., New York, N.Y.
22. **Graf, G. A., W.-P. Li, R. D. Gerard, I. Gelissen, A. White, J. C. Cohen, and H. H. Hobbs.** 2002. Coexpression of ATP-binding cassette proteins ABCG5 and ABCG8 permits their transport to the apical surface. J. Clin. Investig. **110:**659–669.
23. **Gupta, S. D., R. S. Mehan, T. R. Tansey, H. T. Chen, G. Goping, I. Goldberg, and I. Shechter.** 1999. Differential binding of proteins to peroxisomes in rat hepatoma cells: unique association of enzymes involved in isoprenoid metabolism. J. Lipid Res. **40:**1572–1584.
24. **Haave, N. C., and S. M. Innis.** 2001. Cholesterol synthesis and accretion within various tissues of the fetal and neonatal rat. Metabolism **50:**12–18.
25. **Hodge, V. J., S. J. Gould, S. Subramani, H. W. Moser, and S. K. Krisans.** 1991. Normal cholesterol synthesis in human cells requires functional peroxisomes. Biochem. Biophys. Res. Commun. **181:**537–541.
26. **Hogenboom, S., G. J. Romeijn, S. M. Houten, M. Baes, R. J. A. Wanders, and H. R. Waterham.** 2002. Absence of functional peroxisomes does not lead to deficiency of enzymes involved in cholesterol biosynthesis. J. Lipid Res. **43:**90–98.
27. **Horton, J. D., J. L. Goldstein, and M. S. Brown.** 2002. SREBPs: activators of the complete program of cholesterol and fatty acid synthesis in the liver. J. Clin. Investig. **109:**1125–1131.
28. **Ishibashi, S., M. Schwarz, P. K. Frykman, J. Herz, and D. W. Russell.** 1996. Disruption of cholesterol 7α-hydroxylase gene in mice. I. Postnatal lethality reversed by bile acid and vitamin supplementation. J. Biol. Chem. **271:**18017–18023.
29. **Klucken, J., C. Buchler, E. Orso, W. E. Kaminski, M. Porsch-Ozcurumez, G. Liebisch, M. Kapinsky, W. Diederich, W. Drobnik, M. Dean, R. Allikmets, and G. Schmitz.** 2000. ABCG1 (ABC8), the human homolog of the *Drosophila* white gene, is a regulator of macrophage cholesterol and phospholipid transport. Proc. Natl. Acad. Sci. USA **97:**817–822.
30. **Kovacs, W. J., L. M. Olivier, and S. K. Krisans.** 2002. Central role of peroxisomes in isoprenoid biosynthesis. Prog. Lipid Res. **41:**369–391.
31. **Krisans, S. K., J. Ericsson, P. A. Edwards, and G. A. Keller.** 1994. Farnesyl diphosphate synthase is localized in peroxisomes. J. Biol. Chem. **269:**14165–14169.
32. **Lund, E. G., C. Xie, T. Kotti, S. D. Turley, J. M. Dietschy, and D. W. Russell.** 2003. Knockout of the cholesterol 24-hydroxylase gene in mice reveals a brain-specific mechanism of cholesterol turnover. J. Biol. Chem. **278:**22980–22988.
33. **Malle, E., K. Oettl, W. Sattler, G. Hoefler, and G. M. Kostner.** 1995. Cholesterol biosynthesis in dermal fibroblasts from patients with metabolic disorders of peroxisomal origin. Eur. J. Clin. Investig. **25:**59–67.
34. **Mandel, H., M. Getsis, M. Rosenblat, M. Berant, and M. Aviram.** 1995. Reduced cellular cholesterol content in peroxisome-deficient fibroblasts is associated with impaired uptake of the patient's low density lipoprotein and with reduced cholesterol synthesis. J. Lipid Res. **36:**1385–1391.
35. **Miyake, J. H., S.-L. Wang, and R. A. Davis.** 2000. Bile acid induction of cytokine expression by macrophages correlates with repression of hepatic cholesterol 7α-hydroxylase. J. Biol. Chem. **275:**21805–21808.
36. **Miyazawa, S., H. Hayashi, M. Hijikata, N. Ishii, S. Furuta, H. Kagamiyama, T. Osumi, and T. Hashimoto.** 1987. Complete nucleotide sequence of cDNA and predicted amino acid sequence of rat acyl-CoA oxidase. J. Biol. Chem. **262:**8131–8137.
37. **Oettl, K., E. Malle, H. Grillhofer, W. Sattler, and G. M. Kostner.** 1996. Cholesterol metabolism in cells with different peroxisomal defects. Clin. Chim. Acta **251:**131–143.
38. **Oram, J. F., and R. M. Lawn.** 2001. ABCA1. The gatekeeper for eliminating excess tissue cholesterol. J. Lipid Res. **42:**1173–1179.
39. **Osono, Y., L. A. Woollett, J. Herz, and J. M. Dietschy.** 1995. Role of the low density lipoprotein receptor in the flux of cholesterol through the plasma and across the tissues of the mouse. J. Clin. Investig. **95:**1124–1132.
40. **Rachubinski, R. A., and S. Subramani.** 1995. How proteins penetrate peroxisomes. Cell **83:**525–528.
41. **Reddy, J. K., and T. Hashimoto.** 2001. Peroxisomal beta-oxidation and peroxisome proliferator-activated receptor alpha: an adaptive metabolic system. Annu. Rev. Nutr. **21:**193–230.
42. **Repa, J. J., G. Liang, J. Ou, Y. Bashmakov, J. A. Lobaccaro, I. Shimomura, B. Shan, M. S. Brown, J. L. Goldstein, and D. Mangelsdorf.** 2000. Regulation of mouse sterol regulatory element-binding protein-1c gene (SREBP-1c) by oxysterol receptors, LXRa and LXRb. Genes Dev. **14:**2819–2830.
43. **Repa, J. J., E. G. Lund, J. D. Horton, E. Leitersdorf, D. W. Russell, J. M.**

Dietschy, and S. D. Turley. 2000. Disruption of the sterol 27-hydroxylase gene in mice results in hepatomegaly and hypertriglyceridemia. Reversal by cholic acid feeding. J. Biol. Chem. **275:**39685–39692.
44. **Repa, J. J., J. M. Dietschy, and S. D. Turley.** 2002. Inhibition of cholesterol absorption by SCH 58053 in the mouse is not mediated via changes in the expression of mRNA for ABCA1, ABCG5, or ABCG8 in the enterocyte. J. Lipid Res. **43:**1864–1874.
45. **Russell, D. W.** 2003. The enzymes, regulation, and genetics of bile acid synthesis. Annu. Rev. Biochem. **72:**137–174.
46. **Russell, D. W., and K. D. R. Setchell.** 1992. Bile acid biosynthesis. Biochemistry **31:**4737–4749.
47. **Schwarz, M., E. G. Lund, K. D. R. Setchell, H. J. Kayden, J. E. Zerwekh, I. Bjoerkhem, J. Herz, and D. W. Russell.** 1996. Disruption of cholesterol 7α-hydroxylase gene in mice. II. Bile acid deficiency is overcome by induction of oxysterol 7α-hydroxylase. J. Biol. Chem. **271:**18024–18031.
48. **Schwarz, M., E. G. Lund, R. Lathe, I. Björkhem, and D. W. Russell.** 1997. Identification and characterization of a mouse oxysterol 7α-hydroxylase cDNA. J. Biol. Chem. **272:**23995–24001.
49. **Schwarz, M., D. W. Russell, J. M. Dietschy, and S. D. Turley.** 1998. Marked reduction in bile acid synthesis in cholesterol 7a-hydroxylase-deficient mice does not lead to diminished tissue cholesterol turnover or to hypercholesterolemia. J. Lipid Res. **39:**1833–1843.
50. **Stamellos, K. D., J. E. Shackelford, I. Shechter, G. Jiang, D. Conrad, G. A. Keller, and S. K. Krisans.** 1993. Subcellular localization of squalene synthase in rat hepatic cells. J. Biol. Chem. **268:**12825–12836.
51. **Staudinger, J. L., B. Goodwin, S. A. Jones, D. Hawkins-Brown, K. I. MacKenzie, A. LaTour, Y. Liu, C. D. Klaassen, K. K. Brown, J. Reinhard, T. M. Willson, B. H. Koller, and S. A. Kliewer.** 2001. The nuclear receptor PXR is a lithocholic acid sensor that protects against liver toxicity. Proc. Natl. Acad. Sci. USA **98:**3369–3374.
52. **Van Heusden, G. P., J. R. van Beckhoven, R. Thieringer, C. R. Raetz, and K. W. Wirtz.** 1992. Increased cholesterol synthesis in Chinese hamster ovary cells deficient in peroxisomes. Biochim. Biophys. Acta **1126:**81–87.
53. **Vanhorebeek, I., M. Baes, and P. E. Declercq.** 2001. Isoprenoid biosynthesis is not compromised in a Zellweger syndrome mouse model. Biochim. Biophys. Acta **1532:**28–36.
54. **Wanders, R. J. A., and G. J. Romeijn.** 1996. Cholesterol biosynthesis in Zellweger syndrome: normal activity of mevalonate kinase, mevalonate-5-pyrophosphate decarboxylase and IPP-isomerase in patients' fibroblasts but deficient mevalonate kinase activity in liver. J. Inherited Metab. Dis. **19:**193–196.
55. **Woollett, L. A.** 2001. The origins and roles of cholesterol and fatty acids in the fetus. Curr. Opin. Lipidol. **12:**305–312.
56. **Xie, W., A. Radominska-Pandya, Y. Shi, C. M. Simon, M. C. Nelson, E. S. Ong, D. J. Waxman, and R. M. Evans.** 2001. An essential role for nuclear receptors SXR/PXR in detoxification of cholestatic bile acids. Proc. Natl. Acad. Sci. USA **98:**3375–3380.
57. **Yang, T., P. J. Espenshade, M. E. Wright, D. Yabe, Y. Gong, R. Aebersold, J. L. Goldstein, and M. S. Brown.** 2002. Crucial step in cholesterol homeostasis: sterols promote binding of SCAP to INSIG-1, a membrane protein that facilitates retention of SREBPs in ER. Cell **110:**489–500.
58. **Yabe, D., M. S. Brown, and J. L. Goldstein.** 2002. Insig-2, a second endoplasmic reticulum protein that binds SCAP and blocks export of sterol regulatory element-binding proteins. Proc. Natl. Acad. Sci. USA **99:**12753–12758.
59. **Yu, L., J. Li-Hawkins, R. E. Hammer, K. E. Berge, J. D. Horton, J. C. Cohen, and H. H. Hobbs.** 2002. Overexpression of ABCG5 and ABCG8 promotes biliary cholesterol secretion and reduces fractional absorption of dietary cholesterol. J. Clin. Investig. **110:**671–680.